Discovery of a novel allosteric inhibitor scaffold for polyadenosine-diphosphate-ribose polymerase 14 (PARP14) macrodomain 2

Moses Moustakim [a,b,c,j], Kerstin Riedel [d,j], Marion Schuller [a,b], Andrè P. Gehring [d], Octovia P. Monteiro [a,b], Sarah P. Martin [e], Oleg Fedorov [a,b], Jag Heer [f], Darren J. Dixon [c], Jonathan M. Elkins [a,g], Stefan Knapp [h,i], Franz Bracher [d,*], Paul E. Brennan [a,b,*]

[a] Structural Genomics Consortium, University of Oxford, ORCRB, Old Road Campus, Headington, Oxford, Oxfordshire OX3 7DQ, UK
[b] Target Discovery Institute, University of Oxford, NDM Research Building, Old Road Campus, Headington, Oxford, Oxfordshire OX3 7FZ, UK
[c] Department of Chemistry, Chemistry Research Laboratory, University of Oxford, Oxford OX1 3TA, UK
[d] Department of Pharmacy - Center for Drug Research, Ludwig-Maximilians University, Munich 81377, Germany
[e] Charles River, Chesterford Research Park, CB10 1XL, UK
[f] UCB Pharma Ltd, Slough SL1 3WE, UK
[g] Structural Genomics Consortium, Universidade Estadual de Campinas, Cidade Universitária Zeferino Vaz, Campinas, SP 13083-886, Brazil
[h] Johann Wolfgang Goethe-University, Institute for PharmaceuticalChemistry and Buchmann Institute for Life Sciences, Frankfurt am Main 60438, Germany
[i] German Cancer Centre (DKFZ) and DKTK site Frankfurt/Mainz, 60590, Germany

ARTICLE INFO

ABSTRACT

The polyadenosine-diphosphate-ribose polymerase 14 (PARP14) has been implicated in DNA damage response pathways for homologous recombination. PARP14 contains three (ADP ribose binding) macro-domains (MD) whose exact contribution to overall PARP14 function in pathology remains unclear. A medium throughput screen led to the identification of *N*-(2(-9H-carbazol-1-yl)phenyl)acetamide (GeA-69, **1**) as a novel allosteric PARP14 MD2 (second MD of PARP14) inhibitor. We herein report medicinal chemistry around this novel chemotype to afford a sub-micromolar PARP14 MD2 inhibitor. This chemical series provides a novel starting point for further development of PARP14 chemical probes.
© 2018 The Authors. Published by Elsevier Ltd. This is an open access article under the CC BY license (http://creativecommons.org/licenses/by/4.0/).

1. Introduction

Poly-(ADP ribose) Polymerases (PARPs) are ADP-ribosyl transferase enzymes which post-translationally modify substrate proteins.[1] Of at least 17 human family members of PARPs a sub-set, referred to as mono(ADP-ribose)transferases (mARTs), are capable of transferring on a single ADP unit to a given substrate.[2] PARP14 (ARTD8) is the largest of the mARTs and contains multiple domains including an ADP ribose transferase domain (ART), a WWE domain, two (RNA binding) RRM repeats and three (ADP-ribose binding) macrodomains.[3] PARP14 was found to be highly expressed in B-cell lymphoma and hepatocellular carcinoma and has been associated with poor patient prognosis.[4] Furthermore PARP14 has been linked

to inhibition of pro-apoptotic kinase JNK1 which activates pyruvate kinase M2 isoform (PKM2) which in turn promotes a higher rate of glycolysis in cancer (Warburg effect)[5] shown in some contexts to be regulated by high MYC expression.[6] Despite links with cancer pathogenesis[5,7] and inflammatory diseases,[1b,c,7,8] only a few small molecule PARP14 inhibitors have been reported and many have suffered from a lack of selectivity.[9] Most examples of PARP inhibitors have targeted the catalytic domain (ART)[10] such as a recent example by Upton and coworkers who identified moderately selective PARP14 inhibitors,[10e] however to date no PARP14 modulators targeting other domains such as the macrodomains have been reported until recently.[11]

PARP14 contains three macrodomain modules (MD1, MD2 and MD3); biophysical characterisation of macrodomain:ADP-ribsose peptide binding was carried out revealing MD2 as the most potent ADP ribsosyl peptide binding domain and therefore the most likely to deliver a functional effect through small molecule inhibition (PARP14 MD1/ADP-ribose peptide K_D 137 ± 7 μM, PARP14 MD2/ADP-ribose peptide K_D 6.8 ± 0.1 μM, PARP14 MD3/ADP-ribose peptide K_D 15 ± 0.9 μM, Supp. Info Fig. 1 (Fig. 1).

Figure 1. Initial hit PARP14 MD2 inhibitor GeA-69 (**1**) and sulfonamide analogue **2**.

GeA-69 (**1**)
PARP14 MD2 IC$_{50}$ 0.71 μM
PARP14 MD2 K_D (ITC) 0.86 μM

2
PARP14 MD2 IC$_{50}$ 0.9 μM
PARP14 MD2 K_D (ITC) 2.1 μM

1 (X= C)
2 (X= SO)

X= O,NH, S
A–D= Het/Ar
Y=C or SO
R= alkyl, aryl, benzyl, NR'$_2$

Figure 3. SAR studies of carbazoles GeA-69 (**1**) and **2**.

An initial medium throughput screen (∼50 k compounds) revealed compound GeA-69 (**1**) as a sub-micromolar inhibitor of PARP14 MD2 ADP-ribose binding as measured by AlphaScreen™, ITC and BLI.[11a] A co-crystal structure of closely related sulfonamide derivative **2** with PARP14 MD2, which was obtained in the course of the project revealed a unique allosteric binding mode for this inhibitor (PDB ID 5O2D). Overlay of this structure with bound ADP-ribose from a previously published co-crystal structure of PARP14 MD2 (PDB 3Q71)[12] showed that compound **2** occupied a novel pocket adjacent to the binding site for ADP-ribose (Fig. 2A).[11a]

Carbazole **2** engages PARP14 MD2 in a pocket adjacent to the ADP-ribose binding site and the interaction is characterised by a H-bond between the carbazole *N*-H and backbone carbonyl of Pro1130 (*N*-O distance 2.8 Å), an H-bond between one sulfonamide carbonyl and the backbone *N*-H of Ile1132 (O-N distance 2.8 Å), and an H-bond from the sulfonamide *N* to a water molecule in the binding pocket. A comparison of the two structures rationalises inhibitory activity as carbazole **2** induces a shift in the loop region adjacent to Pro1130 which consequently moves into the ADP-ribose binding site (Fig. 2A). Evaluation of the co-crystal structure of carbazole **2** with PARP14 MD2 also revealed the possibility of extending the methanesulfonamide motif into larger substituents exploring peripheral regions of this newly identified allosteric site.

2. Results

2.1. Systematic SAR studies of screening hit GeA-69 (1)

The screening hit GeA-69 (**1**) was part of a focused library from the Bracher lab, originally designed for the improvement of kinase inhibitors derived from the 1-(aminopyrimidyl)-β-carboline alkaloid annomontine.[13] The SAR studies on screening hit GeA-69 (**1**) are described in the following compound library generated as potential PARP14 MD2 inhibitors (Fig. 3). In this library, the β-carboline ring system was replaced by its deaza analogue carbazole, and a number of aromatic and heteroaromatic rings were attached to position 1 (Scheme 1) using Suzuki-Miyaura cross coupling reac-

tions of known 1-bromocarbazole[14] with commercially available or synthesised boronic acids and esters to give compounds **3**–**12** (Scheme 1).

2-Pyridyl compound **13** and 4-pyrimidyl analogue **14** were obtained by regioselective nucleophilic addition of 1,9-dilithiated carbazole (obtained in situ from 1-bromocarbazole and 4 equiv. *tert*-butyllithium) to pyridine and pyrimidine, followed by spontaneous rearomatisation during workup. The obtained (hetero)aryl-carbazoles are shown in Fig. 4.

Unfortunately none of these analogues (compounds **3**–**14**) showed any inhibition of PARP14 MD2. Only a few further modifications of the 1-aryl substituent were performed, whereby all new compounds contained the acetylamino moiety, which was recognised as important for activity in this early stage of the project.

The aza analogue **15** was obtained from *N*-SEM protected 1-bromocarbazole by Masuda borylation at C-1, directly followed by Suzuki-Miyaura cross-coupling with 4-amino-3-bromopyridine, subsequent *N*-acetylation and SEM deprotection, as previously described.[11a] This compound has virtually identical size as the active compound **1**, but interestingly was found to be completely inactive at inhibiting PARP14 MD2 presumably due to the differences in electronics of both molecules. Consequently, this compound could serve as a useful negative control in biochemical experiments. The pyridyl-isomers **16** and **17** were obtained in the same manner using 3-amino-2-chloro- and 3-amino-4-chloropyridine in the cross-coupling reaction (Fig. 5). Furthermore, using Suzuki-Miyaura cross-coupling reactions, the acetylaminophenyl residue was attached to position 1 (Scheme 1) of the β-carboline ring system[15] in order to obtain a ring A aza-analogue **18** and to the canthin-4-one **19** and desaza-canthin-4-one[16] **20** ring systems in order to give analogues bearing tetracyclic core structures (Fig. 5).

An analogue of GeA-69 (**1**) with the acetamido group shifted from the ortho to the meta position at the phenyl ring **21** was prepared by Suzuki-Miyaura cross-coupling of 1-bromocarbazole with 3-aminophenyl boronic acid, followed by *N*-acetylation. Additionally, the complete acetylaminophenyl residue was shifted from *C*-1 to *N*-9, whereby in one example a rigid isomer **22** was obtained,
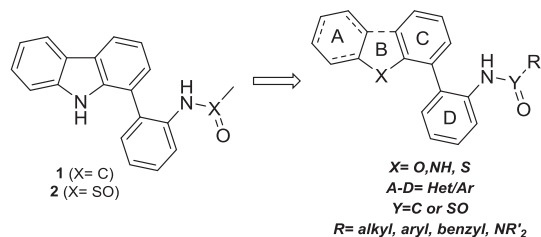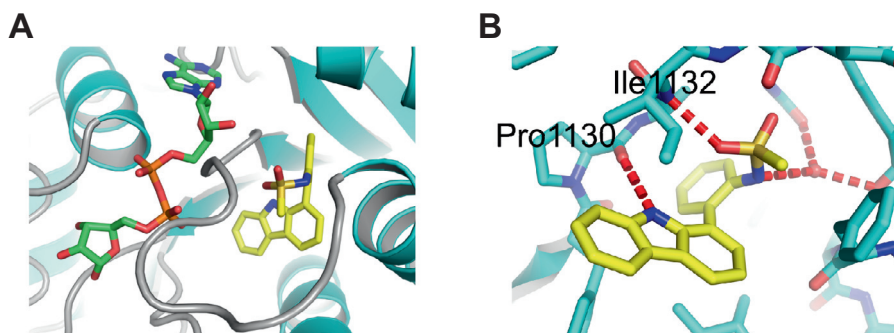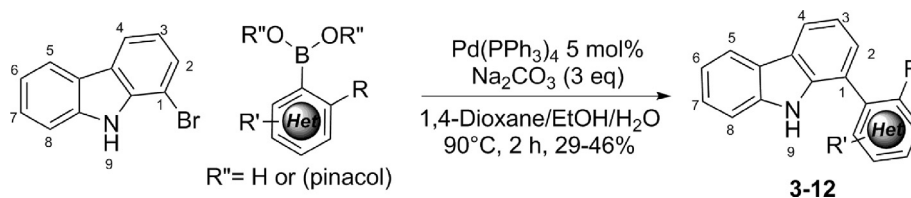

Figure 2. (A) Overlay of bound ADPR (Green sticks) (PDB ID 3Q71) superimposed with PARP14 MD2 (cyan sheets and helices, grey loops): compound **2** (yellow sticks) structure (PDB ID 5O2D). (B) H-Bonding displayed in co-crystal structure of PARP14 MD2 (cyan sticks): compound **2** (yellow sticks) structure (PDB ID 5O2D).

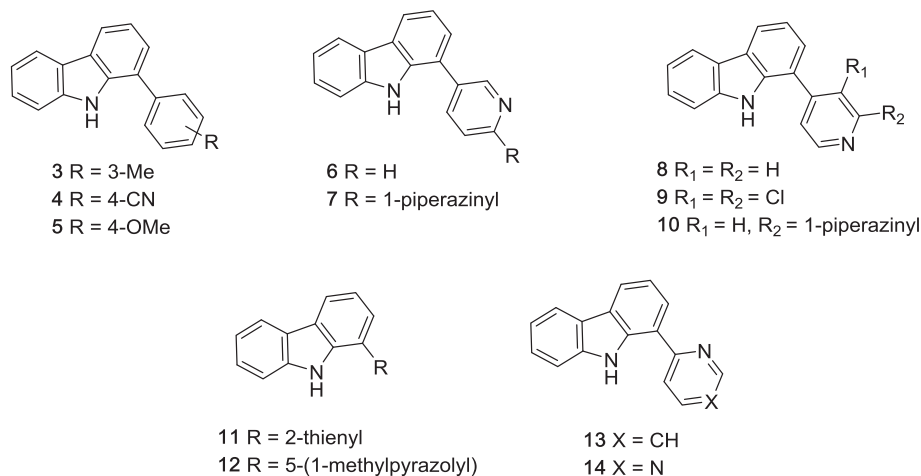**Scheme 1.** Suzuki-Miyaura coupling of 1-bromo-9(H)-carbazole with arylboronic acids or pinacol esters.

3 R = 3-Me
4 R = 4-CN
5 R = 4-OMe

6 R = H
7 R = 1-piperazinyl

8 R_1 = R_2 = H
9 R_1 = R_2 = Cl
10 R_1 = H, R_2 = 1-piperazinyl

11 R = 2-thienyl
12 R = 5-(1-methylpyrazolyl)

13 X = CH
14 X = N

Figure 4. 1-Aryl- and 1-heteroarylcarbazoles **3–14** from the initial compound library. PARP14 MD2 IC$_{50}$ > 50 μM for all compounds.

15
PARP14 MD2 IC$_{50}$ >50 μM

16
PARP14 MD2 IC$_{50}$ >50 μM

17
PARP14 MD2 IC$_{50}$ >50 μM

18
PARP14 MD2 IC$_{50}$ 30 μM

19
PARP14 MD2 IC$_{50}$ >50 μM

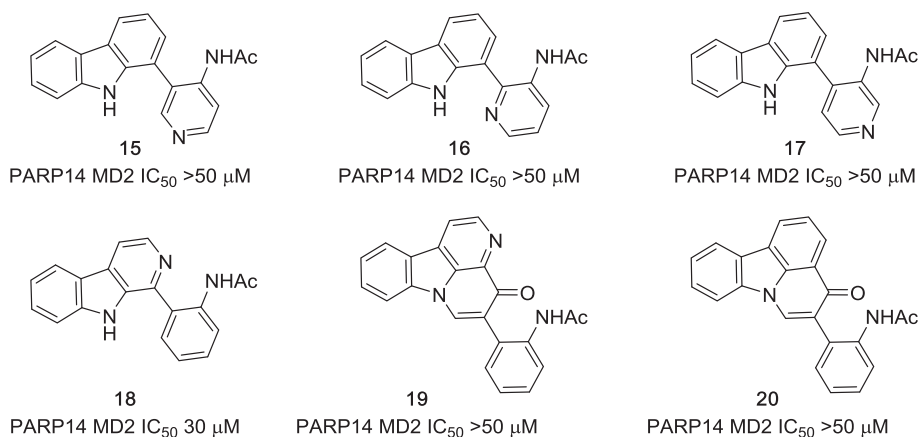20
PARP14 MD2 IC$_{50}$ >50 μM

Figure 5. Aza analogues of screening hit GeA-69 (**1**): compounds **15–18** and analogues bearing tetracyclic core structures canthin-4-one **19**, desazacanthin-4-one **20**.

and in the other, by means of a methylene spacer, a product **23** in which by appropriate rotation both the phenyl and the acetamido group can adopt positions that are very similar to those these groups have in the lead structure GeA-69 (**1**). Compound **22** was obtained by *N*-arylation of carbazole with 2-fluoro-1-nitrobenzene,[17] subsequent reduction of the nitro group, and *N*-acetylation.
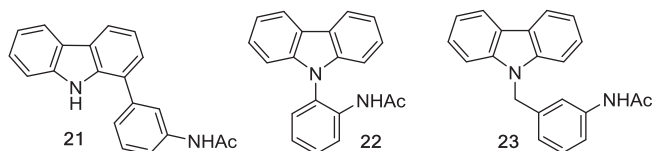

Figure 6. Analogues of GeA-69 (**1**) with the acetylaminophenyl residue shifted to other positions.

N-Benzyl analogue **23** was prepared in an analogous manner via *N*-alkylation of carbazole with 3-nitrobenzyl chloride (Fig. 6).

As modifications of the central pyrrole ring (ring B) of GeA-69 (**1**) *N*-methyl and *N*-benzyl analogues **24** and **25** were prepared starting from corresponding *N*-substituted 1-bromocarbazoles via Suzuki-Miyaura cross-coupling with 2-aminophenylboronic acid and subsequent *N*-acetylation. Dibenzofuran analogue **26** and dibenzothiophene analogue **27** were obtained in a similar manner from commercially available 4-bromodibenzofuran and known 4-iododibenzothiophene (Fig. 7).[18] These experiments were performed before we obtained the crystal structure of PARP14 MD2 with inhibitor **2**, which demonstrated the relevance of the pyrrole NH-group (Fig. 2).

In order to replace the NH group of ring B with either an alternative hydrogen bond donor (hydroxy group) or a hydrogen bond acceptor (carbonyl group), known 1-iodofluorenone[19] was coupled
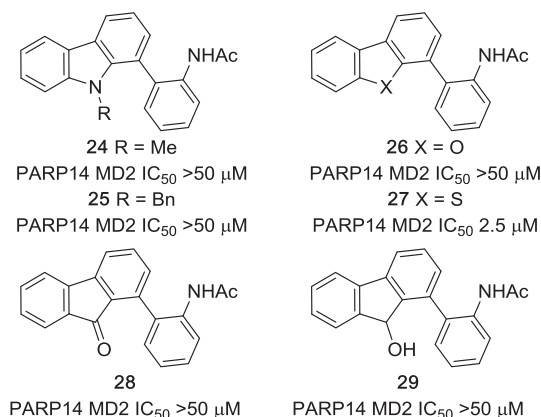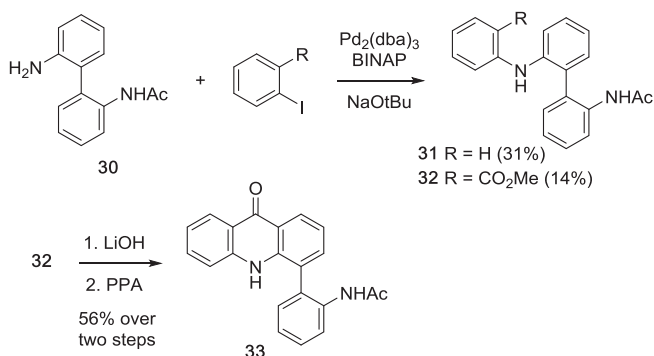
Figure 7. Analogues of GeA-69 (**1**) bearing substituents an *N*-9, as well as dibenzofuran (**26**), dibenzothiophene (**27**), fluorenone (**28**), and fluorenol (**29**) analogues.
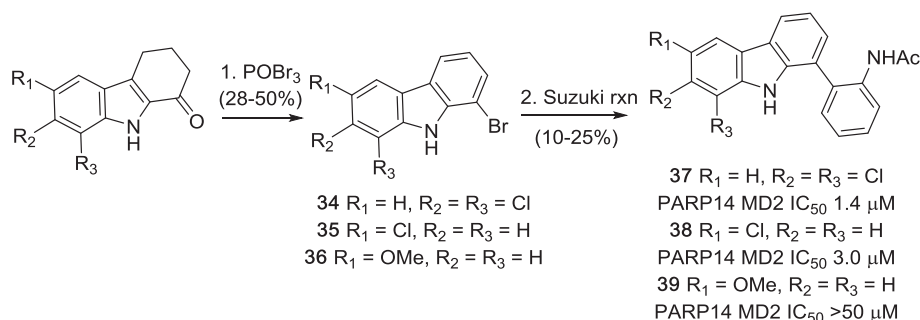

Scheme 2. Synthesis of seco analogue **31** and acridone analogue **33**.
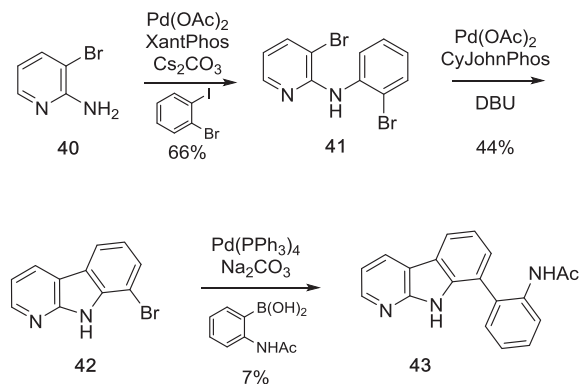
in the established manner to give the 1-arylfluorenone **28** which was easily reduced to the racemic fluorenol **29** with sodium borohydride (Fig. 7).

Controlled mono-acetylation of 2,2′-diaminobiphenyl with equimolar amounts of acetic anhydride gave monoamide **30** in moderate yield. Monoamide **30** was then used to access the seco analogue **31** and the acridone analogue **33**. Buchwald-Hartwig arylation of the unsubstituted anilino group with iodobenzene to give biaryl **31** and with methyl 2-iodobenzoate to give biaryl **32**, respectively, was accomplished with the BINAP/Pd$_2$(dba)$_3$ catalyst system. Ester **32** was hydrolysed to give the corresponding carboxylic acid, which was converted into the acridone **33** by polyphosphoric acid-mediated intramolecular acylation (Scheme 2).[20]

Further, a series of modifications of ring A was performed. Ring-substituted analogues **37–39** were obtained in two steps from


Scheme 4. Synthesis of an 8-aza analogue **43** of GeA-69 (**1**).

readily available 1,2,3,4-tetrahydrocarbazol-1-ones[21] **34–36** in two steps. Treatment of the ketones with POBr$_3$ in anisole gave the corresponding 1-bromocarbazoles under bromination/dehydrogenation conditions in moderate to poor yields. Subsequent standard Suzuki-Miyaura cross-coupling gave the desired arylcarbazoles **37–39** (Scheme 3).

8-Aza analogue **43** was obtained by a series of three consecutive Pd-catalyzed coupling reactions.[22] Chemoselective Buchwald-Hartwig amination of 1-bromo-2-iodobenzene with 2-amino-3-bromopyridine **40** using XantPhos as a ligand gave phenylaminopyridine **41**, which was cyclised to 8-bromo-α-carboline **42** using CyJohnPhos in an intramolecular Heck coupling. Finally, the acetylaminophenyl residue was introduced in a standard Suzuki-Miyaura cross-coupling (Scheme 4).

Analogue **44** bearing a partially hydrogenated A-ring was obtained from the corresponding brominated tetrahydrocarbazole[23] via Suzuki-Miyaura cross-coupling. A truncated analogue, the 7-aryl-3-isopropylindole **45**, in which ring C is replaced by an isopropyl group, was obtained by Suzuki-Miyaura cross-coupling of the respective 7-bromoindole. The 6-aza-5,6,7,8-tetrahydro analogue **47** was prepared in a similar manner from known intermediate **46**.[24] Improved yields were obtained, if the secondary amine was protected with the Boc group prior to the cross-coupling reaction (Scheme 5).

Finally, modifications of the acetamido group located at the 1-phenyl substituent (ring D) were performed. Aminophenyl intermediate **48** was further converted into the urea analogue **49** by treatment with *tert*-butyl isocyanate (Scheme 6). Since α-trifluoroethylamines are known as bioisosteres of amide groups from peptide chemistry,[25] we also prepared compound **51** for SAR studies. Intermediate **48** was thus converted into 1,1,1-trifluoropropan-2-imine **50** by Pd-catalysed cross-coupling with 2-bromo-3,3,3-trifluoro-1-propene;[26] subsequent reduction with sodium borohydride gave the racemic target compound **51**. Treat-

Scheme 3. Synthesis of analogues of of GeA-69 (**1**) bearing additional substituents at ring A.
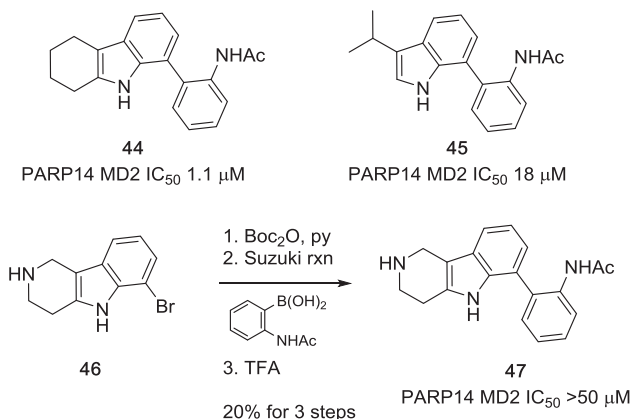
Scheme 5. Analogues of GeA-69 (**1**) with partially hydrogenated or truncated ring A.
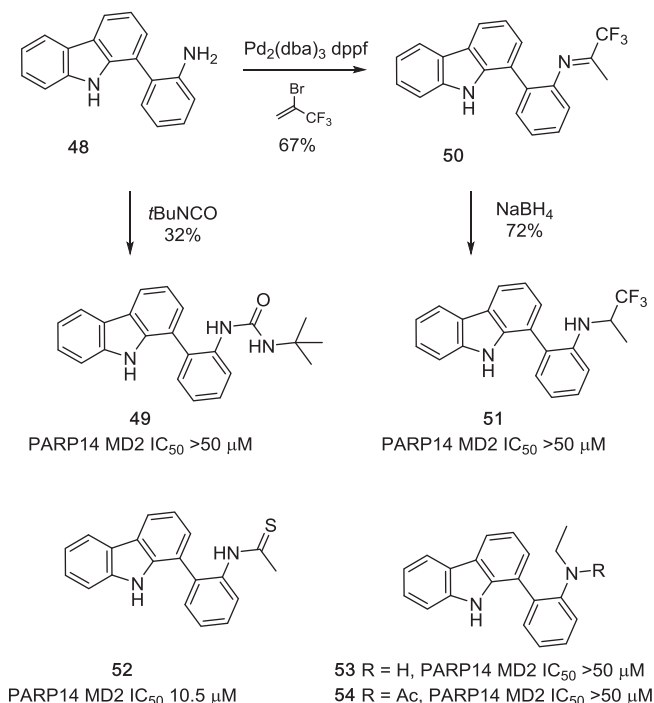
Scheme 6. Variations of the acetamide group (thioamide **52**, reduced *N*-ethylamine **53**, *N*-ethyl analogue **54**, urea analogue **49**). Synthesis of the proposed amide bioisoster **51** from aniline **48**.

ment of GeA-69 (**1**) with Lawesson's reagent gave the thioamide analogue **52**. Reduction of the amide group in **1** with borane-disulfide yielded the *N*-ethyl analogue **53**, which in turn could be *N*-acetylated to give the *N*-ethyl acetamide **54**.

A screening of the above presented compounds on PARP14 MD2 clearly demonstrated that lead structure GeA-69 (**1**) is very sensitive to structural modifications. Carbazoles bearing (hetero)aromatic residues different from the acetylaminophenyl residue of GeA-69 (**1**) (Figure 4) were found to be inactive. Analogues with almost identical shape albeit very different electronically (aza analogues in the rings A, C and D) are completely or virtually (β-carboline **18**, IC$_{50}$ 30 µM) inactive. Any changes in the central pyrrole ring (ring B) eliminated inhibitory activity as well. The NH group was found to be essential, it can not be replaced by another hydrogen bond donor, as demonstrated by the inactive fluorenol analogue, **29**. Surprisingly, the dibenzothiophene analogue **27** showed considerable inhibition (IC$_{50}$ 2.5 µM),

whereas the dibenzofuran, **26** and the acridone, **33** were inactive. The same holds for the (deaza)compounds having tetracyclic canthin-4-one backbones (canthin-4-one **19**, deazacanthin-4-one **20**). The seco analogue of GeA-69 (**1**), biaryl **31**, was completely inactive, demonstrating that not only the presence of the functional groups of the lead structure, but also their fixation by the carbazole backbone is most important.

The tetrahydro-analogue **44** showed only a slight loss in activity (IC$_{50}$ 1.1 µM) compared to GeA-69 (**1**), whereas its 6-aza analogue **47** bearing a polar aliphatic amino group in ring A, was inactive. Lipophilic chlorine substituents at ring A (compounds **37–38**) were fairly tolerated (IC$_{50}$ 1.4 and 3.0 µM), but the 6-methoxy analogue **39** was inactive. These observations can be rationalised by the hydrophobic environment in the binding region of ring A consisting of residues V1032, V1092, M1108, I111, I1112, F1129, I1132 (Fig. 2).

Removal of the *N*-acetyl residue from GeA-69 (**1**), conversion of the acetamide into a tertiary amide **54** or into the proposed trifluoroalkyl bioisoster **51**, as well as reduction of the amide moiety to an amine **53** resulted in complete loss of activity, the thioamide **52** was an order of magnitude less active (IC$_{50}$ 10.5 µM) than GeA-69 (**1**).

In conclusion, these data confirm a very narrow structure-activity relationship for rings A-C (Fig. 3), and for further optimisation of the screening hit GeA-69 (**1**) only modifications of either the *N*-acyl residue or ring D were deemed promising.

2.2. SAR studies of ring D and N-acyl residues

Initial construction of the carbazole series was performed using 1-bromo-9*H*-carbazole and a series of pinacol boronic esters which were coupled under standard Suzuki-Miyaura conditions, furnishing biaryl products in moderate to good yields (Scheme 1). A number of these compounds were then converted to the corresponding acetamides or methanesulfonamides and profiled for their binding activity with PARP14 MD2. Whilst binding activity was not improved, additional substituents on ring D such as methyl, fluoro and cyano were tolerated maintaining single digit µM activity (compounds **55–57**, Table 1). As previously observed a comparison of these compounds with the inactive non-acetylated and non-sulfonylated anilines (eg compounds **59–61**, Table 1) showed the requirement of this group for binding activity.

Further modification of biaryl-amine **48** to the corresponding amides or sulfonamides (Scheme 7) was carried out. The corresponding amides and sulfonamides **62–108** were then profiled for their PARP14 MD2 binding affinity (Tables 1 and 2).
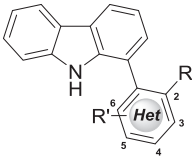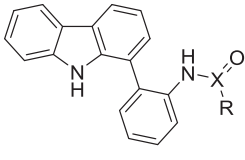
Compounds were profiled for binding activity with PARP14 MD2 through a competitive (AlphaScreen™) binding assay measuring the displacement of ADP-ribose peptide from PARP14 MD2.[11a] Promising compounds were additionally profiled by biophysical assays such as Bio-Layer Interferometry or Isothermal Titration Calorimetry as previously described.[11a]

As previously described the parent carbazole GeA-69 (**1**) was profiled for its broader selectivity over 12 other human macrodomains, showing exquisite selectivity for MD2 of PARP14.[11a] Furthermore a representative selectivity screen of 46 kinases in a Differential Scanning Calorimetry assay did not reveal any significant activity of carbazole GeA-69 (**1**) at 10 µM.[11a]

3. Discussion

The binding activities of synthesised PARP14 MD2 inhibitors are summarised in Tables 1 and 2. Despite comprehensive SAR studies of the A-C rings of this carbazole series, no points for the development of more potent ligands were discovered, a number of deriva-

Table 1
Binding affinity characterisation data of carbazole series for PARP14 MD2.

#	R	R'	IC$_{50}$ (μM)	K$_D$ (μM)	#	R	X	IC$_{50}$ (μM)
1 (GeA-69)	**-NHAc**	**H**	**0.72 ± 0.04**	**0.86** ± 0.04	66	-Et	C	1.0 ± 0.03
2	-NHSO$_2$Me	H	0.9 ± 0.09	2.1 ± 0.1	67	*n*-Pr	C	0.9 ± 0.04
17	-NHAc	3-aza	>50	n.d.	68	*n*-Bu	C	>50
49	-NHC(O)NH-*t*Bu	H	7.2 ± 1.4	n.d.	69	-CH$_2$CH$_2$OMe	SO	8.6 ± 0.4
52	-NHC(S)CH$_3$	H	10.5 ± 0.4	n.d.	70	5-Methylisoxazo-4-yl	SO	>50
53	-NHEt	H	>50	n.d.	71	-NMe$_2$	SO	2.5 ± 0.1
54	-NEtAc	H	>50	n.d.	72	Ph	SO	>50
55	-NHSO$_2$Me	4-Me	1.1 ± 0.1	n.d.	73	-CF$_3$	C	1.1 ± 0.07
56	-NHSO$_2$Me	4-CN	n.d.[a]	5.2 ± 1.7	74	-Cyclopropyl	C	1.2 ± 0.03
57	-NHAc	6-Me	1.7 ± 0.1	1.6 ± 0.7	75	-Cyclohexyl	C	>50
58	-NHSO$_2$Me	5-CF$_3$	>50	n.d.	76	-2-furyl	C	>50
59	-NH$_2$	4-Me	>50	n.d.	77	-Ph	C	1.9 ± 0.07
60	-NH$_2$	5-CF$_3$	>50	n.d.	78	**-CH$_2$Ph**	**C**	**7.6 ± 0.3**
61	-NH$_2$	6-Me	>50	n.d.	79	**-CH$_2$Ph**	**SO**	**3.6 ± 0.3**
62	-NHSO$_2$Et	H	1.2 ± 0.03	n.d.	80	2-OMe-Ph	C	>50
63	-NHSO$_2$*n*-Pr	H	2.9 ± 0.1	n.d.	81	3-OMe-Ph	C	12.7 ± 1.5
64	-NHSO$_2$*n*-Bu	H	3.3 ± 0.1	n.d.	82	4-OMe-Ph	C	9.0 ± 1.4
65	-NHC(O)CH$_2$NMe$_2$	H	5.5 ± 0.6	n.d.				

[a] Data was not successfully obtained due to solubility issues in the AlphaScreen assay with this example.
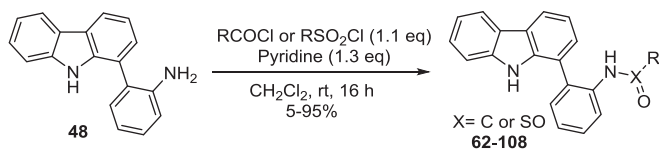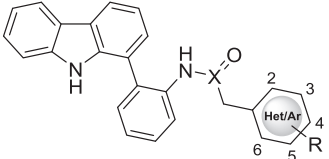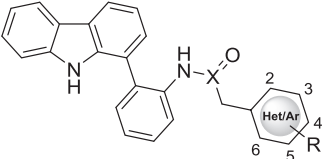

Scheme 7. Synthesis of amide and sulfonamide derivatives of aniline **48**.

tives were synthesised functionalising ring D (Figure 3). Only small additional substituents to the ring were tolerated (e.g. compounds **55–57**, Table 1). Interestingly, elaboration of the sulfonamide in compound **2** into the homologated ethane-, propane- and butane-sulfonamides analogues (compounds **62–64**, Table 1) furnished equipotent compounds. Further elaboration of the acetamide in GeA-69 (**1**) mostly retained single digit μM binding activity (eg compounds **66**,**67**). Interestingly the *n*-pentanoyl analogue **68** was seemingly inactive, which may be due the entropic penalty associated with longer alkyl substituents or a steric clash with the protein. However, guided by the apparent tolerance of some larger substituents in place of the acetamide in GeA-69 (**1**) and methanesulfonamide in compound **2**, the 2-phenylacetamide and phenylmethanesulfonamide of compounds **78** and **79** (IC$_{50}$ 7.6 ± 0.3 and 3.6 ± 0.3 μM respectively, Table 1) were chosen for further development as they enabled rapid access to diversity and provide a suitable vector for binding pocket exploration. A number of hetero- and substituted- aromatics were appended onto the biaryl core (examples **83–108**, Table 2). Moderately flat SAR was observed for both 2- and 4- substituted phenylacetyl and phenylmethanesulfonamide groups. It was found that introduction of a 3-cyano substituent in the phenylmethanesulfonamide series provided a slight improvement in binding activity compared with GeA-69 (**1**). Carbazole **108** displays sub-micromolar activity for

Table 2
Binding affinity characterisation data of carbazole series for PARP14 MD2.

#	R/Het	X	IC$_{50}$ (μM)[a]	K$_D$ (μM)	#	R/Het	X	IC$_{50}$ (μM)[a]
83	3-aza	C	1.1	1.5[a]	96	4-Cl	C	6.2 ± 0.6
84	3-aza-4-Me	C	1.0	2.7[a]	97	4-CF$_3$	SO	8.1 ± 0.7
85	3, 6-aza	C	2.1 ± 0.1	3.9[a]	98	3,4-OMe	C	4.3 ± 0.3
86	4-aza-3-CN	C	2.4 ± 0.2	n.d.	99	3,4-dioxole	C	6.9 ± 0.6
87	3-aza-4-CN	C	3.5 ± 0.2	n.d.	100	2-F-5-CN	SO	1.2 ± 0.0 (K$_D$ 1.3 ± 0.51)
88	3-aza-4-OH	C	6.6 ± 0.4	n.d.	101	2,5-Me	C	44.6 ± 10.4
89	2-F	SO	2.4 ± 0.1	n.d.	102	3,4-Cl	C	6.3 ± 0.6
90	2-F	C	2.8 ± 0.2	n.d.	103	3-OMe	C	6.6 ± 0.5
91	2-Cl	C	4.4 ± 0.3	n.d.	104	3-F	C	4.2 ± 0.3
92	4-Me	C	8.7 ± 1.2	n.d.	105	3-F	SO	1.4 ± 0.1
93	4-F	C	>50	n.d.	106	3-CF$_3$	C	7.1 ± 0.7
94	4-OMe	C	6.2 ± 0.6	n.d.	107	3-CN	C	2.1 ± 0.1
95	4-CN	SO	6.2 ± 0.6	n.d.	108	**3-CN**	**SO**	**0.66 ± 0.03** (K$_D$ 0.55 ± 0.22)

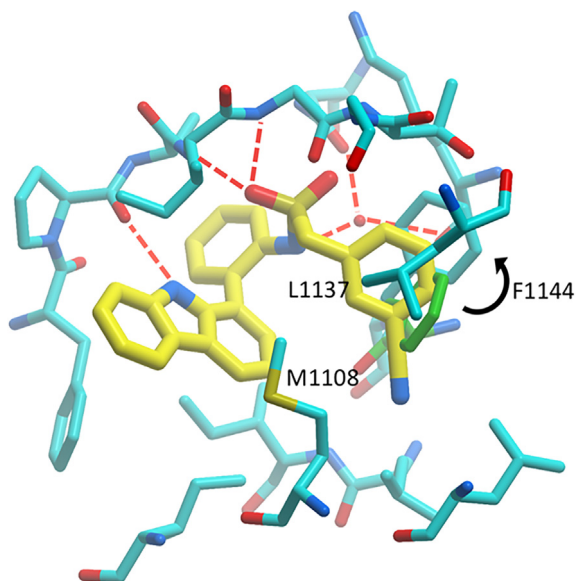[a] No error of fit obtained for these K$_D$ values. n.d. denotes not determined.

Figure 8. Flexible side-chain docking studies of carbazole **108** with PARP14 MD2 (from PDB ID 5O2D) reveal new potential hydrophobic interactions with M1108, L1137 and F1144 after rotation of F1144 (black arrow, conformation in PDB ID 5O2D shown in green sticks) to accommodate the 3-cyanophenyl group.

PARP14 MD2 (IC$_{50}$ 660 ± 30 nM). Notably, by comparison the corresponding 3-cyanophenylacetamide **107** displays diminished binding activity relative to sulfonamide **108**, potentially due to the greater tolerance of the sulfonamide to maintaining H-bond acceptor interactions as shown in the PARP14 MD2:compound **2** co-crystal structure (Fig. 2B). The 3-cyanobenzyl group of compound **108** may make interactions with adjacent hydrophobic residues M1108, L1137 and F1144. Although we were unable to obtain a co-crystal structure of compound **108** to confirm these interactions, we performed docking studies to examine possible binding modes of the larger compound compared to compound **2**. Simple minimisation of compound **108** in PARP14 MD2 is unable to find a binding pose due to clashes between the larger 3-cyanophenyl group and the protein. To account for potential side chain rotations that would be necessary to accommodate this group, we performed SCARE docking (SCan Alanines and Refine) using ICM.[27] The optimised pose for compound **108** shows a rotation of the side chain of F1144 to open up space so that the 3-cyanophenyl group can make interactions with M1108 and L1137 in addition to a pi-stacking interaction with F1144 (Fig. 8). However, it is not obvious from this docking study why the 3-cyanophenyl group would be preferred to other hydrophobic groups such as in compounds **79** and **83–107**.

Sub-micromolar PARP14 MD2 affinity of carbazole **108** was also confirmed by BioLayer Interferometry (BLI) providing a calculated K_D of 550 nM ± 220. Whilst lead compound **108** is larger and a less ligand efficient inhibitor of PARP14 MD2 than original hit compound **1**, owing to the more tolerant SAR around it represents an attractive chemical starting point for future development. Additional examples similar to compound **108** (see SI, compounds **109–116**) have been explored and work to improve the binding activity and physicochemical properties of this lead molecule will be reported in due course.

4. Summary

We herein report the development of a novel class of allosteric modulators of the second macrodomain of PARP14. Initial identification of carbazole GeA-69 (**1**) as a submicromolar inhibitor of PARP14 MD2 was made following a medium throughput screen.[11a]

Inhibitory activity can be rationalised through a PARP14 MD2 co-crystal of a similar derivative, sulfonamide **2** (PDB ID 5O2D). Investigation into this carbazole series was then made revealing new opportunities for ligand elaboration. Systematic analysis of SAR demonstrated a very narrow structure activity relationship for rings A-C (carbazole scaffold), and for further optimisation of the screening hit **1** only modifications of either the *N*-acyl residue or ring D showed promise. A number of carbazole containing compounds were tolerated in this newly identified allosteric site of PARP14 MD2 including a 3–cyano substituted phenylmethanesulfonamide **108**. Carbazole **108** displays submicromolar activity binding to PARP14 MD2 by AlphaScreen (IC$_{50}$ 0.66 µM) which was also confirmed by BLI (K_D 0.55 µM). This lead molecule along with others in this series are useful chemical starting points in the development of chemical probes for this poorly understood epigenetic target.

A. Supplementary data

Supplementary data associated with this article can be found, in the online version, at https://doi.org/10.1016/j.bmc.2018.03.020.

References

1. (a) Gibson BA, Kraus WL. New insights into the molecular and cellular functions of poly(ADP-ribose) and PARPs. *Nat Rev Mol Cell Biol*. 2012;13:411–424;
   (b) Rack JGM, Perina D, Ahel I. Macrodomains: Structure, Function, Evolution, and Catalytic Activities. *Annu Rev Biochem*. 2016;85:431–454;
   (c) Wahlberg E, Karlberg T, Kouznetsova E, et al. Family-wide chemical profiling and structural analysis of PARP and tankyrase inhibitors. *Nat Biotech*. 2012;30:283–288.
2. (a) Kleine H, Poreba E, Lesniewicz K, et al. Substrate-Assisted Catalysis by PARP10 Limits Its Activity to Mono-ADP-Ribosylation. *Mol Cell*. 2008;32:57–69;
   (b) Ame J-C, Spenlehauer C, de Murcia G. The PARP superfamily. *BioEssays*. 2004;26:882–893;
   (c) Vyas S, Matic I, Uchima L, et al. Family-wide analysis of poly(ADP-ribose) polymerase activity. *Nat Commun*. 2014;5:4426.
3. Hottiger MO, Hassa PO, Lüscher B, Schüler H, Koch-Nolte F. Toward a unified nomenclature for mammalian ADP-ribosyltransferases. *Trends Biochem Sci*. 2010;35:208–219.
4. Yamashita T, Ji J, Budhu A, et al. EpCAM-positive hepatocellular carcinoma cells are tumor-initiating cells with stem/progenitor cell features. *Gastroenterology*. 2009;136:1012–1024.
5. Iansante V, Choy PM, Fung SW, et al. PARP14 promotes the Warburg effect in hepatocellular carcinoma by inhibiting JNK1-dependent PKM2 phosphorylation and activation. *Nat Commun*. 2015;6:7882.
6. Mushtaq M, Darekar S, Klein G, Kashuba E. Different Mechanisms of Regulation of the Warburg Effect in Lymphoblastoid and Burkitt Lymphoma Cells. *PLoS ONE*. 2015;10:e0136142.
7. (a) Barbarulo A, Iansante V, Chaidos A, et al. Poly(ADP-ribose) polymerase family member 14 (PARP14) is a novel effector of the JNK2-dependent pro-survival signal in multiple myeloma. *Oncogene*. 2013;32:4231–4242;
   (b) Cho SH, Ahn AK, Bhargava P, et al. Glycolytic rate and lymphomagenesis depend on PARP14, an ADP ribosyltransferase of the B aggressive lymphoma (BAL) family. *Proc Natl Acad Sci USA*. 2011;108(38):15972–15977.

8. Han W, Li X, Fu X. The macro domain protein family: Structure, functions, and their potential therapeutic implications. *Mutat Res Rev Mutat Res.* 2011;727:86–103.

9. (a) Sonnenblick A, de Azambuja E, Azim Jr HA, Piccart M. An update on PARP inhibitors-moving to the adjuvant setting. *Nat Rev Clin Oncol.* 2015;12:27–41;
   (b) Lord CJ, Ashworth A. PARP inhibitors: Synthetic lethality in the clinic. *Science.* 2017;355:1152–1158.

10. (a) Peng B, Thorsell A-G, Karlberg T, Schüler H, Yao SQ. Small Molecule Microarray Based Discovery of PARP14 Inhibitors. *Angew Chem Int Ed.* 2017;56:248–253;
    (b) Andersson CD, Karlberg T, Ekblad T, et al. Discovery of Ligands for ADP-Ribosyltransferases via Docking-Based Virtual Screening. *J Med Chem.* 2012;55:7706–7718;
    (c) Wang P, Li J, Jiang X, et al. Palladium-catalyzed N-arylation of 2-aminobenzothiazole-4-carboxylates/carboxamides: facile synthesis of PARP14 inhibitors. *Tetrahedron.* 2014;70:5666–5673;
    (d) Ekblad T, Lindgren AEG, Andersson CD, et al. Towards small molecule inhibitors of mono-ADP-ribosyltransferases. *Eur J Med Chem.* 2015;95:546–551;
    (e) Upton K, Meyers M, Thorsell A-G, et al. Design and synthesis of potent inhibitors of the mono(ADP-ribosyl)transferase, PARP14. *Bioorg Med Chem Lett.* 2017;27:2907–2911.

11. (a) Schuller M, Riedel K, Gibbs-Seymour I, et al. Discovery of a Selective Allosteric Inhibitor Targeting Macrodomain 2 of Polyadenosine-Diphosphate-Ribose Polymerase 14. *ACS Chem Biol.* 2017;12:2866–2874(b) Haikarainen T, Maksimainen MM, Obaji E, Lehtiö L. Development of an Inhibitor Screening Assay for Mono-ADP-Ribosyl Hydrolyzing Macrodomains Using AlphaScreen Technology. *SLAS DISCOVERY: Adv. Life Sci. R&D* 0(0):2472555217737006.(c) Ekblad T, Verheugd P, Lindgren AE, Nyman T, Elofsson M, Schüler H. Identification of Poly(ADP-Ribose) Polymerase Macrodomain Inhibitors Using an AlphaScreen Protocol. *SLAS DISCOVERY: Adv. Life Sci. R&D* 0 (0):2472555217750870.

12. Forst AH, Karlberg T, Herzog N, et al. Recognition of Mono-ADP-Ribosylated ARTD10 Substrates by ARTD8 Macrodomains. *Structure.* 2013;21:462–475.

13. (a) Bracher F, Hildebrand D. β-Carbolin-Alkaloide, II Tributyl(1-ethoxyvinyl) stannan als C2-Baustein für die Synthese von β-Carbolin-Alkaloiden. *Liebigs Ann.* 1993;1993:837–839;
    (b) Stroedke B, Gehring AP, Bracher F. Synthesis of Desaza Analogues of Annomontine and Canthin-4-one Alkaloids. *Arch Pharm.* 2015;348:125–131;
    (c) Kern S, Agarwal S, Huber K, et al. Inhibition of the SR Protein-Phosphorylating CLK Kinases of Plasmodium falciparum Impairs Blood Stage Replication and Malaria Transmission. *PLoS ONE.* 2014;9:e105732.

14. Strödke B, Gehring AP, Bracher F. Synthesis of Desaza Analogues of Annomontine and Canthin-4-one Alkaloids. *Arch Pharm (Weinheim).* 2015;348:125–131.

15. Bracher F, Hildebrand D. 1,9-Dimetalated ß-carbolines. Versatile building blocks for the total synthesis of Alkaloids. *Tetrahedron.* 1994;50:12329–12336.

16. Tremmel T, Puzik A, Gehring AP, Bracher F. Canthin-4-ones as Novel Antibacterial Agents. *Arch Pharm (Weinheim).* 2016;349:710–723.

17. Wharton SI, Henry JB, McNab H, Mount AR. The Production and Characterisation of Novel Conducting Redox-Active Oligomeric Thin Films From Electrooxidised Indolo[3,2,1-jk]carbazole. *Chem Eur J.* 2009;15:5482–5490.

18. Amara R, Bentabed-Ababsa G, Hedidi M, et al. Synthesis of N-Aryl and N-Heteroaryl γ-, δ-, and ε-Lactams Using Deprotometalation-Iodination and N-Arylation, and Properties Thereof. *Synthesis.* 2017;28:4500–4516.

19. Tilly D, Samanta SS, Castanet A-S, De A, Mortier J. The Expedient and Regioselective Metalation of Unprotected Biphenyl-2-, -3-, and -4-carboxylic Acids. *Eur J Org Chem.* 2006;2006:174–182.

20. Watterson SH, Chen P, Zhao Y, et al. Acridone-Based Inhibitors of Inosine 5'-Monophosphate Dehydrogenase: Discovery and SAR Leading to the Identification of N-(2-(6-(4-Ethylpiperazin-1-yl)pyridin-3-yl)propan-2-yl)-2-fluoro-9-oxo-9,10-dihydroacridine-3-carboxamide (BMS-566419). *J Med Chem.* 2007;50:3730–3742.

21. Gehring AP, Bracher F. A Convenient Conversion of Substituted Cyclohexenones into Aryl Methyl Ketones. *Synthesis.* 2012;44:2441–2447.

22. Mineno M, Sera M, Ueda T, et al. Rapid access to diverse α-carbolines through sequential transition metal catalyzed amination and direct C-H arylation. *Tetrahedron.* 2014;70:5550–5557.

23. Barclay BM, Campbell N. 135. Dehydrogenation of tetrahydrocarbazoles by chloranil. *J Chem Soc.* 1945;530–533.

24. Dossetter AG, Beeley H, Bowyer J, et al. (1R,2R)-N-(1-Cyanocyclopropyl)-2-(6-methoxy-1,3,4,5-tetrahydropyrido[4,3-b]indole-2-carbonyl)cyclohexanecarboxamide (AZD4996): A Potent and Highly Selective Cathepsin K Inhibitor for the Treatment of Osteoarthritis. *J Med Chem.* 2012;55:6363–6374.

25. (a) Meanwell NA. Synopsis of Some Recent Tactical Application of Bioisosteres in Drug Design. *J Med Chem.* 2011;54:2529–2591;
    (b) Deutsch A, Glas H, Hoffmann-Roder A, Deutsch C. Synthesis of functionalized α-trifluoroethyl amine scaffolds via Grignard addition to N-aryl hemiaminal ethers. *RSC Adv.* 2014;4:9288–9291.

26. Kino T, Nagase Y, Horino Y, Yamakawa T. Pd-catalyzed coupling of arylamines and 2-bromo-3,3,3-trifluoropropene. *J Mol Catal A Chem.* 2008;282:34–51.

27. Bottegoni G, Kufareva I, Totrov M, Abagyan R. A new method for ligand docking to flexible receptors by dual alanine scanning and refinement (SCARE). *J Comput Aided Mol Des.* 2008;22:311–325.